Nat Hazards (2011) 59:1691–1714
DOI 10.1007/s11069-011-9860-2

ORIGINAL PAPER

Identification of potentially dangerous glacial lakes in the northern Tien Shan

Tobias Bolch · Juliane Peters · Alexandr Yegorov · Biswajeet Pradhan · Manfred Buchroithner · Victor Blagoveshchensky

Received: 13 April 2010 / Accepted: 17 May 2011 / Published online: 22 June 2011

Abstract Like in many other parts of the world, the glaciers in northern Tien Shan are receding, and the permafrost is thawing. Concomitantly, glacial lakes are developing. Historically, outbursts of these glacial lakes have resulted in severe hazards for infrastructures and livelihood. Multi-temporal space imageries are an ideal means to study and monitor glaciers and glacial lakes over large areas. Geomorphometric analysis and modelling allows to estimate the potential danger for glacial lake outburst floods (GLOFs). This paper presents a comprehensive approach by coupling of remote sensing, geomorphometric analyses aided with GIS modelling for the identification of potentially dangerous glacial lakes. We suggest a classification scheme based on an additive ratio scale in order to prioritise sites for detailed investigations. The identification and monitoring of glacial lakes was carried out semi-automatically using band ratioing and the normalised difference water index (NDWI) based on multi-temporal space imagery from the years 1971 to 2008 using Corona, ASTER and Landsat data. The results were manually edited when required. The probability of the growth of a glacial lake was estimated by analysing glacier changes, glacier motion and slope analysis. A permafrost model was developed based on geomorphometric parameters, solar radiation and regionalised temperature conditions which permitted to assess the influence of potential permafrost thawing. Finally, a GIS-based model was applied to simulate the possibly affected area of lake outbursts. The findings of this study indicate an increasing number and area of glacial lakes in the northern Tien Shan region. We identified several lakes with a medium to high potential for an outburst after a

T. Bolch (✉)
Geographisches Institut, Universität Zürich, 8059 Zürich, Switzerland
e-mail: tobias.bolch@geo.uzh.ch

T. Bolch · J. Peters · B. Pradhan · M. Buchroithner
Institut für Kartographie, Technische Universität Dresden, 01062 Dresden, Germany

A. Yegorov · V. Blagoveshchensky
Institute of Geography of Ministry of Education and Sciences of the Republic of Kazakhstan, Almaty, Kazakhstan

B. Pradhan
Institute of Advanced Technology, University Putra Malaysia, UPM, 43400 Serdang, Malaysia

classification according to their outburst probability and their downstream impact. These lakes should be investigated more in detail.

Keywords Glacial lakes · GLOF · Debris-flow · Remote sensing · Geomatics · GIS · Modelling · Hazard assessment · Tien Shan

1 Introduction

Climate change and concomitant glacier recession has caused the development and expansion of glacial lakes in mountain areas of the world which leads to an increasing risk of lake outbursts. Outbursts of glacial lakes represent a serious hazard especially for populated regions in the mountains all over the world (Clague and Evans 2000; Huggel et al. 2003, 2005; Iwata et al. 2002; Ma et al. 2004; Popov 1988; Richardson and Reynolds 2000). These glacial lake outburst floods (GLOF, also called jökullhlaup) can cause extremely high water discharges as well as large mudflow events. Triggering events for an outburst can be moraine failures induced by an earthquake, by the degradation of permafrost and increased water pressure, or a rock, snow, or ice avalanche into the lake causing a flood wave with a subsequent outburst (Buchroithner et al. 1982; Fujita et al. 2008; Ives 1986; Vuichard and Zimmermann 1987). The potential downstream path has to be taken into account in order to asses the potential effect of a GLOF event on the infrastructure and human population. Previous studies showed that the susceptibility of lake development is highest where the glaciers have a low surface slope angle and a low flow velocity or are stagnant (Bolch et al. 2008; Frey et al. 2010a; Quincey et al. 2007; Reynolds 2000).

Glacial lakes that develop in remote mountainous areas are often difficult to access and field studies are laborious and cost-intensive. Therefore, remote sensing data and GIS are ideal tools for studying and monitoring glacial lakes and assessing their hazard potential (Buchroithner 1996; Huggel et al. 2003; Schneider 2004; Kääb et al. 2005; Quincey et al. 2005; Bolch et al. 2008).

Recently, several studies demonstrated the suitability of optical remote sensing data for detection of glacial lakes in an automated way (Huggel et al. 2002; Quincey et al. 2005; Bolch et al. 2008; Frey et al. 2010a). The aforementioned literature review indicates that one of the main drawbacks in the automated methods is the difficulty in differentiating the lakes with turbid water and the fact that the areas with cast shadow are usually misclassified. While the latter can be addressed by applying a shadow mask using a precise digital elevation model (Huggel et al. 2002), so far no real promising method for turbid water is existing in the literature. Hence, manual checking and editing is still essential. Manual digitizing is also required for panchromatic data such as aerial imagery and declassified intelligence data such as Corona.

A digital elevation model (DEM) of the study area is essential to obtain the geomorphometric data of the glaciers, glacial lakes and its surroundings and especially for modelling of the probable outburst path. The freely available near-global void-filled SRTM3 DEM and the ASTER GDEM are a good choice if no other detailed local DEM is available (Frey et al. 2010b). The SRTM3 DEM and ASTER derived DEMs were shown to be suitable with the limitation that the elevation and characteristics of smaller features such as the lateral moraines and deep gorges may not be accurately and precisely depicted (Fujita et al. 2008; Huggel et al. 2003; Kamp et al. 2005). Additional errors occur especially on steep slopes due to low contrast in areas with cast shadow in the utilised imagery (GDEM) and layover and foreshortening of the radar data (SRTM DEM, Kocak et al. 2004). Reported RSME values are <15 m for mountainous terrain (Berry et al. 2007; Falorni et al. 2005).

Table 1 Examples of past GLOF events in northern Tien Shan and their triggering factors

Date	Location	Elevation (m)	Discharge volume (m^3)	Transported volume	Cause/trigger	Reference
15/07/1973	Proglacial lake, Kishi Almaty	3,370	~180,000	~4 mio m^3	Over filling of the lake kettle; high surface discharge over the dam, dam erosion	Baimoldayev and Vinohodov (2007) Plehanov et al. (1975)
03/08/1977	Khumbel river basin right inflow of Ulken Almaty	3,400	~200,000	~4 mio m^3	Superficial discharge initiated by lake overfilling	Popov (1984a)
21/06/1979	Srednij Talgar	3,400	~80,000	~113,000 m^3	Subglacial tunnel	Shusharin and Popov (1981)
23/07/1980	Kaskelen river basin	3,500	~200,000	~2 mio m^3	Tunnel in buried ice	Popov (1984b)

The northern Tien Shan is prone to natural hazards due to gravitative processes such as avalanches, landslides, debris flows and flash floods (Havenith et al. 2003; Passmore et al. 2008; Severskiy and Zichu 2000; Storm and Korup 2006; Yegorov 2007). Several catastrophic mudflows have been documented during the last 100 years and before (Gorbunov and Severskiy 2001; Blagoveshchenskiy and Yegorov 2009, Table 1). It has been shown that about 11% of the catastrophic mudflows were triggered by GLOFs (Popov 1988; Medeuov and Nurlanov 1996; Medeuov et al. 1993, Yegorov 2007).

The aim of this study is to investigate the suitability of a comprehensive geomatics-based approach to detect and monitor potential dangerous glacial lakes (PDGL) in the northern Tien Shan and classify the glacial lakes according to their hazard potential. Hence, we address level 1 (basic detection of glacial lakes) and level 2 (assessment of hazard potential) based on the multi-level strategy as suggested by Huggel et al. (2002). A further aim is to recommend which lakes should be further investigated using high resolution imagery and in the field (level 3). Addressing the risk for the society of a GLOF event is beyond the scope of this study. The utilised approach should be based on standardised criteria, sophisticated yet rather simple and suitable for assessing a large number of glaciers simultaneously. The conditioning parameters which influence the potential danger of a glacial lake are widely published in some of the aforementioned papers on GLOFs. The interpretation, however, is mainly based on description or subjective classification. The analysis presented here uses the above mentioned conditioning parameters and is more objective.

2 Study area

The mountain ranges Ile Alatau and Kungöj Ala–Too (also: Zailijskij and Kungej Alatau, 42°30′–43°30′N, 75°–79°E) of the northern Tien Shan are located in Central Asia at the border between Kazakhstan and Kyrgyzstan (Fig. 1). These ranges rise from the Kazakh Steppe at an elevation of about 800 m asl to nearly 5,000 m asl. The southern edge is an intra-mountainous basin filled by Lake Issyk–Kul (also: Isyk–Köl, 1,608 m asl). Many villages, the million habitant city of Almaty and important tourist destinations such as Cholpon–Ata at lake Issyk–Kul as well as major roads are situated directly at the foothills of these mountains.

The mountain chain of the northern Tien Shan originate from the Caledonian orogenesis but are still affected by compression and are still slightly uplifting. The area is situated within the Chilik–Kemin Seismic Zone (Chedija 1986; Utirov 1978) with several predominant WSW–ENE-striking faults.

The appearance of the seismically active mountain ranges is mainly formed by neotectonic activity (Chedija 1986). Several major earthquakes have occurred since the end of the 19th century and thousands of smaller seismic events have been recorded (Lukk et al. 1995). The major earthquake of the year 1887 ($M_s = 7.3$) affected the large town Almaty (called Vernyi at that time) situated at the edge of Ile Alatau (Yadav and Kulieshhius 1992). Another major earthquake (Kemin earthquake, $M_s = 8.2$) occurred in 1911 and caused numerous landslides and rock avalanches in northern Tien Shan (Delevaux et al. 2001). Moreover, evidence of several prehistoric earthquakes also exists in this region (Korjenkov et al. 2004).

Due to the topography, the overall continental climate is characterised by distinct local variability. Precipitation at altitudes about 3,000 m asl ranges from more than 1,000 mm/a on windward northern slopes to less than 800 mm in a leeward valley south of the main mountain ridges (Bolch 2007). The minimum precipitation occurs in the study area during winter due to the Siberian anticyclone and the maximum occurs in early summer due to both cyclonic activity and convective precipitation (Böhner 1996). Mean annual air temperature (MAAT) recorded at Tuyuksu glacier station (3,434 m asl) is about −4°C. The zero degree isotherm is situated just above 2,700 m asl. The steady-state equilibrium line altitude of glaciers is situated at about 3,800 m asl on northern slopes and between 3,900 and 4,000 m asl on southern slopes (Bolch 2007). A characteristic feature of the northern Tien Shan is its pronounced periglacial zone with many large and active rock glaciers. This

Fig. 1 Location of the study area

zone is characterised by frequent diurnal freeze–thaw cycles (Marchenko 1999). Permafrost is sporadic at about 2,700–3,200 m asl, discontinuous at 3,200–3,500 m asl, and continuous above 3,500 m asl (Gorbunov et al. 1996). Hence, the drained lakes discussed above were situated in the discontinuous permafrost zone.

3 Data and methods

3.1 Data

Important data used in this study are remote sensing imagery from different time periods (Table 2). The earliest available remote sensing data are Corona and Landsat MSS from the 1970s while the recent data are ASTER and Landsat ETM+ SLCoff (with data gaps due to a scan-line error). Fortunately, larger parts of the study region are within the central part of the SLCoff scenes and are thus not or only partly affected by the gaps.

Most of the utilised scenes show little seasonal snow cover and are therefore suitable for lake and glacier identification. Only the ASTER scene from 13/10/2001 showed the presence of larger snow cover. Nevertheless, it was used as supplementary information as most of the lakes are identifiable. Unfortunately, no suitable scene from the 1990s was available for this study. Soviet topographical maps with the scale, 1:100,000 from the 1980s and GPS points obtained during multiple fieldworks in the years 2001–2004 were used for orthorectification of the master image (Landsat ETM+, 1999). All other images were co-registered to this image. The void-filled SRTM3 DEM, vers. 4 from CGIAR was used (srtm.csi.cgiar.org/) for rectification. The geometry of the Corona imagery is complex with the least distortion in the centre of the image (Dashora et al. 2007). Fortunately, the area of interest is located around this centre and hence, the distortion is found to be low. For co-registration purposes, a projective transformation followed by rubber sheeting was used in ERDAS Imagine 9.1. The latter was necessary to improve the accuracy which is caused by panoramic distortion. The overall $RMS_{x,y}$ error is less than two Landsat pixels (~56 m, Table 2) which is acceptable considering the complex image geometry and the mountainous terrain. The $RMS_{x,y}$ of the other imagery was lower, mostly in the range of one Landsat TM pixel (~30 m, Table 2). The void-filled SRTM3 DEM was also used for the modelling (e.g. mass movements, probable outburst path). The reported accuracy for the SRTM DEM proved true for the study area (Bolch et al. 2005; Bolch 2008).

Table 2 List of satellite data used in this study

Time period	Date	Satellite and sensor	Resolution	Source	$RMS_{x,y}$	Spectral bands
1971/1972	17/09/1971	Corona KH-4B	~5 m	USGS	56 m	PAN
	07/09/1972	Landsat MSS	60 m (res.)	GLCF	47 m	VIS, NIR
~2000	08/08/1999	Landsat ETM+	15 m/30 m	USGS	Reference	VIS, NIR, SWIR
	13/10/2000	Terra ASTER	15 m	USGS	64 m	VIS, NIR, SWIR
	05/09/2001	Terra ASTER	15 m	USGS	40	VIS, NIR, SWIR
	30/09/2001	Terra ASTER	15 m	USGS	41	VIS, NIR, SWIR
~2007	14/08/2007	Landsat SLCoff	15 m/30 m	USGS	21	VIS, NIR, SWIR
	13/06/2008	Landsat SLCoff	15 m/30 m	USGS	11	VIS, NIR, SWIR

3.2 Glacial lake identification

Water reflects mainly within the visible spectrum with a maximum value in the green band. This typical characteristic enables to identify the clean water using multi-spectral imagery. We tested several methods like ratioing and the normalised differenced water index (NDWI) with different band combinations (e.g. Blue, Green, NIR, SWIR). The main aim was to obtain the most precise delineation of lakes with some ice on the water and turbid lakes with minimum misclassification error. The best results were obtained using the NDWI approach by employing NIR and Blue or NIR and Green bands. The water index using Blue performed better in the shaded areas while the index with Green had lesser problems with ice on the water bodies. Finally, the NDWI was used by employing NIR and Green bands (Green − NIR/Green + NIR). The utilised thresholds were adapted for each of the individual scene (Table 3). The misclassified shadow areas were eliminated using a shadow mask (Huggel et al. 2002). Hence, few lakes in shadow had to be digitised manually. The procedure for the lake identification is shown by Figure 2.

Table 3 Overview of the utilised NDWI thresholds for different sensors

	Landsat MSS	ASTER	Landsat ETM+
Threshold	0.45–0.9	0.3–0.7	0.3–0.9

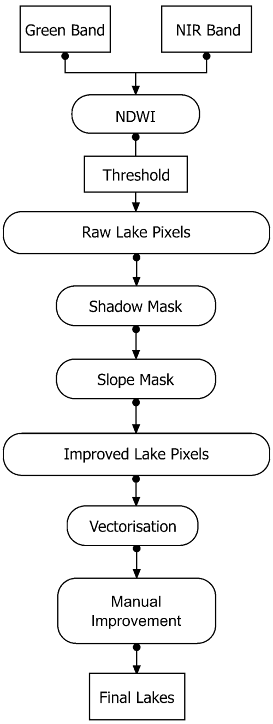

Fig. 2 Procedure showing automated lake identification

The delineated water bodies with the coarser resolution of MSS were manually improved using the Corona data. An image stretching algorithm was used in order to facilitate the visual detection of water bodies in the panchromatic Corona images. The position of some lakes did not match perfectly with MSS images due to the distortion of the Corona images. In this case, the lakes were completely digitised from the Corona imagery and manually shifted in order to match with the correct position in the MSS data. Not all glacial lakes could be identified on each image. This largely depended on the image quality. Presence of shadow and especially snow cover hampers the identification of high altitude lakes. On the other hand, some lakes might have disappeared due to slow lake drainage or a sudden outburst.

Apart from the quality of the scene, sources of possible errors are attributed to the accuracy of the lake delineation and the error during co-registration. The highest $RMSE_{x,y}$ in co-registration is about 50 m (Table 2). However, as we compared the absolute change in area and not the exact location, therefore the impact of this on the derived data is relatively negligible. The remaining errors were estimated based on a buffer method using similar approach as suggested by Granshaw and Fountain (2006). Half a pixel was chosen as the buffer size as this is supposed to represent the worst possible case in which all margin pixels were wrongly classified. This method also includes relatively higher error of smaller polygons as those may have a higher number of edge pixels.

3.3 Hazard assessment

Several factors need to be taken into account when assessing the hazard potential of a glacial lake outburst. In this study, the methodology of Huggel et al. (2002) and Bolch et al. (2008) was adapted and expanded as we introduce a higher number of variables for hazard assessment. The hazard assessment can be summarised by four major parameter groups: lake characteristics, characteristics of the lake surroundings, characteristics of the adjacent glaciers, impact on downstream areas. Each of those groups consists of several variables. Table 4 gives an overview of the addressed variables and its applicability using remote sensing and references for this task.

3.3.1 Lake characteristics

One of the most important variables for analysing the potential danger of a GLOF is the change of the glacial lake. We address the issue of changes based on space imagery from three different time periods (Table 4). The growth of a supraglacial or proglacial lake depends primarily on the glacier characteristics and retreat. We expanded the analysis on glacier shrinkage based on Bolch (2007, 2008) and include the glacier area of 2007 for those lakes adjacent to a glacier. The volume of the lakes is addressed based on the empirical formula (Eq. 1) suggested by Huggel et al. (2002) which is primarily based on 15 lakes with existing depth measurements.

$$V = 0.104 A^{1.42} \tag{1}$$

However, it is important to highlight here that this scaling formula may only serve as a first estimation only as the lake volume depends on several variables. By applying this formula, (Eq. 1) for the lakes in Kishi Almaty valley with existing measurements of the bathymetry (Kasatkin and Kapista 2009; Tokmagambetov 2009) reveals an overestimation of the volume of up to 20% (Lake no. 1: modelled value: 33,040 m^3, measured value

Table 4 Key factors contributing to the hazard risk of a glacial lake and its investigation using remote sensing data (based on Richardson and Reynolds 2000; Huggel et al. 2002; Quincey et al. 2005; Bolch et al. 2008)

Characteristics group	Factor	Remote sensing data source and applicable techniques	Suitable for automatisation	References
Lake characteristics	Lake area and volume	Detection using multi-temporal multi-spectral (MS) satellite data	Yes	Wessels et al. (2002), Huggel et al. (2002)
	Rate of lake formation and growth	Change detection using multi-temporal (MT) and MS satellite data	Yes	Bolch et al. (2008)
Glacier characteristics	Fluctuations of the glacier	Investigation of area and volume change of the glacier based on MS and MT satellite data, MT digital elevation models (DEMs)	Yes	Bolch et al. (2010, 2011), Paul et al. (2002), Aizen et al. (2006)
	Activity of the glacier	Derive glacier velocity using feature tracking or DInSAR based on MT optical or radar data	Yes	Kääb (2005), Luckman et al. (2007), Scherler et al. (2008), Bolch et al. (2008)
	Geomorphometric characteristics of the glacier	Geomorphometric DEM analysis, slope classification	Yes	Bolch et al. (2007), Quincey et al. (2005)
Characteristics of the lake surrounding	Freeboard between lake and crest of moraine ridge	Geomorphometric DEM analysis	Partly	
	Width and height of the moraine dam	Geomorphometric DEM analysis	Partly	
	Stability of the moraine dam/presence of dead ice in the moraine dam	Investigation of surface deformation based on MT DEM analysis, permafrost modelling	Partly	Fujita et al. (2008)
	Possibility of mass movements into the lakes	Mapping of ice cover and geology using MS data, Geomorphometric DEM analysis of the surrounding catchment areas, flow modelling	Yes	Huggel et al. (2003), Salzmann et al. (2004), Allen et al. (2009)
Impact of an GLOF to downstream areas	Affected area	Flow modelling	Yes	Huggel et al. (2003), Mergili et al. (2011)
	Infrastucture down-valley	Detection of human infrastructure based on MS satellite data analysis.	Partly	

27,618 m^3, lake no. 9: 21,563, 17,165 m^3). Similar uncertainty was also mentioned by Huggel et al. (2002).

3.3.2 Characteristics of adjacent glaciers

The recent glaciers were delineated based on the 2007 and 2008 Landsat ETM+ data (Table 2) using band ratioing (Band 4/Band 5) approach in order to be consistent with the method used by Bolch (2007) for the 1999 ETM+ scene. The glacier velocity was estimated from multi-temporal optical imagery based on feature tracking using cross-correlation techniques (Berthier et al. 2005; Bolch et al. 2008; Kääb 2005). Unfortunately, no suitable ASTER data were available. Hence, we chose Landsat scenes from 1999, 2007 and 2008 and used the near infrared band due to the better contrast than in the higher resolution panchromatic band. The open source software 'Cosi–Corr' (Leprince et al. 2007) was applied for the automated estimation of the velocity. This software proved to be well suitable for mountain glaciers (Scherler et al. 2008). Here, it should be noted that Cosi–Corr was developed and applied for imagery from pushbroom scanners such as SPOT and ASTER with known image geometry while Landsat TM/ETM+ data has some inaccuracies in this respect. However, this affects the obtained results only marginally as the main interest here is to know about the activity and not the absolute values of the glacier movement. We estimate a glacier to be stagnant at the snout if the calculated velocity is below the uncertainty of one pixel (30 m/year).

The slope of the glacier surface gives a hint where glacial lakes can develop or an existing lake can extend in the near future. A threshold of 2° for supraglacial lake formation on debris-covered glaciers in the Himalaya (Quincey et al. 2007; Reynolds 2000; cf Bolch et al. 2008) or 5° for the formation of proglacial lakes in overdeepenings of debris-free glaciers in the Alps (Frey et al. 2010b) have been suggested. We applied a slope threshold of 5° as only very few glaciers in the study area have larger portions of debris cover.

3.3.3 Characteristics of lake surroundings

Mass movements like rock fall or ice avalanches into a lake are important triggering mechanisms for an outburst. Hence, an analysis of the surrounding topography is highly sought after. We applied the modified single-flow model (MSF, Huggel et al. 2003) which was developed to model mass movements like debris flows and ice avalanches based on the surrounding topography. The model is a modified D8 flow direction algorithm and calculates the likelihood that a raster cell will be affected by such a mass movement. Similar methods to model rock and ice avalanches were applied by Allen et al. (2009) and Salzmann et al. (2004). Unfortunately, no detailed ground information is available for the study area. Hence, we chose to model the probability of a rock fall based on Kaibori et al. (1988) who presented detailed statistics for the slope at the detachment zone and for the angle of friction. The angle of friction defines the average slope between the starting and end points of the mass movement (Hsü 1975). In contrast to the results of Kaibori et al. (1988) who chose average values, we estimated the minimum values so that 90% of all occurred events are included. The threshold values are 30° for the slope at the detachment zone and 25° for the angle of friction (Table 5). We modelled ice avalanches in a similar way but chose the thresholds to be 25° and 17° based on the empirical work of Alean (1985, Fig. 3a). Although the utilised values are based on studies in the Alps and high mountains in Japan, and may be slightly different for the northern Tien Shan these values seem to be reasonable

Table 5 Parameters and their thresholds used for modelling of the probability of mass movements

Parameter	Rock avalanche (Kaibori et al. 1988)	Ice avalanche (Alean 1985)	Debris flow (Haeberli 1983, Huggel et al. 2002)	Flood wave (Allen et al. 2009)
Minimum slope at the detachment/starting zone	30°	25°	0°	0°
Angle of friction (average incline)	20°	17°	11°	3°

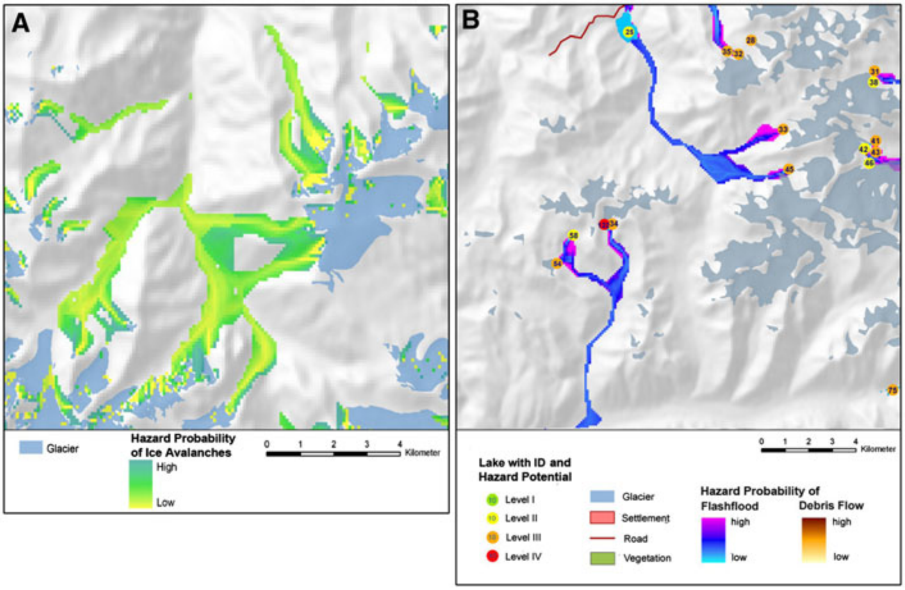

Fig. 3 Examples from the flow modelling. **a** Probability of an area affected by ice avalanches, **b** probability of an area affected by flash floods and mudflows

for estimation as they represent a worst case scenario. For example, Alean (1985) suggested a threshold of 45° for the slope of the detachment zone for cold glaciers and 25° for warm glaciers. Most of the glaciers of the study area are, however, either cold or polythermal. Van der Woerd et al. (2004) estimated a slope of about 45° for the origin of ice avalanches for cold glaciers in the Central Asian Kunlun Shan.

The probability of a dam failure mainly depends on the characteristics of the lake dam itself. In the study area, most of the lake dams comprise morainic materials. The width and height of the dam as well as the freeboard between the lake level and the crest can be visually determined by means of a high resolution DEM and satellite imagery. The available SRTM can provide a hint but the resolution is too coarse for detailed investigations (Fujita et al. 2008). A dam can become unstable if it contains permafrost or buried ice which thaws or will thaw due to changing temperature conditions (Richardson and Reynolds 2000). Comparison of multi-temporal high resolution DEMs can give a hint at the thawing of the ice content and the extent of the lowering of the dam can also be detected (Fujita et al. 2008). However, multi-temporal DEMs of suitable resolution were not available for this study.

In order to obtain some measure whether the moraine dam is currently within the permafrost zone and could be affected by thawing, we modelled the permafrost using a simple empirical model based on Permakart (Keller 1992). This model is based on empirical findings of the permafrost distribution as well as geomorphometric parameters; mean annual air temperature (MAAT) which can be computed using a DEM and additional data. We extended this model and included the solar radiation as additional information. We used the regionalisation of the MAAT as suggested by Bolch (2007, 2008) and the limits of the permafrost distribution (sporadic: 2,700 m asl, discontinuous: 3,200, and continuous: 3,500 m asl, Gorbunov et al. 1996). The physical model by Marchenko (2001) developed for a small subset of the study area (Kishi and Ulken Almaty valley) served as an evaluation dataset. Overall, the model showed a good agreement with the results obtained by Marchenko (2001), but small-scale variability (e.g. caused by the land cover) could not be captured. Climate change had also an impact on the permafrost distribution and permafrost area diminished during the last 130 years (Marchenko et al. 2007). We consider that a dam may become unstable if it is outside the continuous permafrost area. Although being a rough estimation, especially when taking into account that the blocky morainic material itself may retard thawing (Gorbunov et al. 2004) this approach provides a relatively quick estimation about the possible current existence and condition of permafrost in the moraine dam (Fig. 4).

3.3.4 *Impact of glacial lake outburst floods*

A GLOF presents a risk if human life and infrastructures would be affected. Therefore, the probability was calculated to which the downstream area would be affected by a GLOF

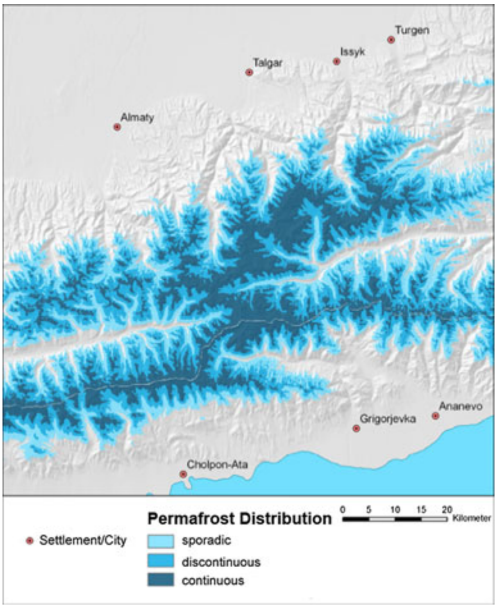

Fig. 4 Modelled permafrost extend

using the previously mentioned MSF model introduced by Huggel et al. (2003). Flash-floods in the Tien Shan and elsewhere often lead to debris flows. Besides the presence of loose sediments, a certain velocity of the water is needed to transport the debris. This again depends mainly on the steepness of slope. In this research, the values for a debris flow were adopted based on the findings of Haeberli (1983) and Huggel et al. (2002) who suggested that the debris flow ends if an average incline of 11° is reached. We estimated that flash flood would occur when the angle of friction is lower than this threshold and stopped the calculation at an angle of friction of less than 3° (Allen et al. 2009, Table 5). However, these thresholds are rough estimations and in reality transitions exist with different flow types occurring in the same event.

As a result, the relative probabilities of an affected downstream area can be calculated (Fig. 3b). A major decisive parameter is the quality of the applied DEM. Therefore, the existing infrastructures are visually interpreted based on the satellite imagery in addition to the existing data of the Tien–Shan–GIS (major roads, settlements, Bolch 2008) for verification.

3.4 Identification of potentially dangerous glacial lakes

In order to be able to identify potentially dangerous glacial lakes in an automated and a most objective way, it is necessary to combine the above mentioned conditioning parameters. We suggest a numerical approach on the basis of additive ratio scales similar to those utilised in business studies (Kahle 1998). The general workflow is presented in Fig. 5. The aim in this context is to have an efficient tool to help to make decisions (e.g. to find the right location(s) for the new business centre). In this case, this approach helps to find out which lakes are potentially of high danger and should be further investigated. For this, each introduced variable has to be tested if it applies to the investigated lake. If so (e.g. if a potential ice avalanche would reach a lake or a lake is in direct contact to the glacier), a value of one (1) is assigned to the lake otherwise a zero (0). However, this approach is not applicable for the lake area and lake growth. A larger lake area usually contains more water and can therefore cause higher damage. We introduced three classes (small, medium, large) and assign 0.5, 1 and 1.5 to each lake according to its area (Table 6). We do not differentiate further as this would usually require subjective interpretation which we want to avoid so that the approach can be utilised for a large number of lakes. The lake growth was treated in a similar way (Table 6).

Ideally, the utilised variables should be independent. This is the case with most of the variables we choose but there are some exceptions: For example, a flash flood will always occur if a mudflow is modelled. Therefor we introduced the precondition factor that a flash flood is only considered if a mudflow did not occur. Also, the increase of lake area depends at least partly on the glacier retreat if a glacier is in direct contact to the glacier. Glacier flow velocity and the variable slope below 5° is also not independent. We considered these two issues while assigning the weighting factors to each variable. A weighting scheme is also needed in order to account for the different impacts on the potential danger of the investigated lakes. However, the weighting is often subjective and depends also on the special situation in the study area.

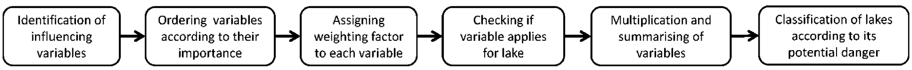

Fig. 5 General workflow for the classification of potential dangerous glacial lakes

Table 6 Weight factors of the selected variables

Variable	Weight factor	
Lake area change	0.1661	0: Shrinkage or no significant growth 0.5: growth <50% of the initial area 1: growth <100% of the initial area 1.5: growth <150% of the initial area 2: growth >150% of the initial area
Risk of ice avalanche	0.1510	1: Modelled deposits hit lake 0: Modelled deposits do not hit lake
Risk of rock fall/avalanche	0.1359	1: Modelled deposits hit lake 0: Modelled deposits do not hit lake
Instable dam[a]	0.1208	1: Dam is within discontinuous permafrost 0: Dam is outside discontinuous permafrost
Debris flow	0.1057	1: Debris flow would occur if an outburst would happen 0: Debris flow would not occur if an outburst would happen
Flash flood	0.0906	1: Flash flood would occur if an outburst would happen 0: Flash flood would not occur if an outburst would happen
Contact to glacier	0.0755	1: Lake is in direct contact with glacier 0: Lake is not in direct contact with glacier
Lake area	0.0604	0.5: Small (size <50,000 m^2) 1.0: Medium (>50,000 and <100,000 m^2) 1.5: Large (>100,000 m^2)
Glacier shrinkage	0.0453	1: Significant glacier shrinkage 0: No significant glacier shrinkage
Glacier slope <5° at the terminus	0.0302	1: Glacier has slope angels below 5° adjacent to the lake 0: Glacier has slope angels above 5° adjacent to the lake
Stagnant ice at the terminus	0.0151	1: No significant glacier velocity was detected at terminus 0: Significant glacier velocity was detected at the terminus
Sum of the weights	1.000	

[a] Although an unstable dam is one of the most important parameter for the potentially danger lake, we consider a lower weighting as we can only address roughly the thawing of permafrost based on the permafrost model

We suggest a weighting scheme after a sequential order of the parameters as this is most objective and each variable is treated separately. The first and crucial step for the suggested scheme is the ordering of the variables after the estimated hazard potential from the highest to the lowest. We considered the knowledge from literature and past GLOF events (Table 1) for this step. Then, the weights are linearly distributed while the 2nd lowest weight is two times the lowest weight, the 3rd lowest is the sum of the 2nd lowest plus the lowest weight and so on. The sum of the weighting factor is set to 1 by default (Table 6). The variables which were applied for each lake are then multiplied with the weighting factor and subsequently added up. Thereafter, a total of nine remote sensing data derived parameters were included and modelled in GIS environment for the current situation, and two additional parameters are also included which indicate whether the glacial lake may continue to grow in the near future.

The characteristics of the moraine dams (width, height, freeboard) could only be addressed visually while other critical measures of the dam stability such as material composition or piping can hardly be addressed from remote sensing. The importance of those is included in the discussion section.

The final classification was established by the definition of qualitative threshold values ranging from very low potential danger to a high danger. The calculated values for the lakes range between 0.03 and 0.88. A very low hazard potential should have a lake only if no or only one factor with low weight applies to the lake. Hence, we choose 0.1 as the first threshold. We consider a lake can be potentially of high danger if the four most important factors apply to the lake or a combination of several factors reaching the sum of the weights of the four most important factors (in our case 0.574). The threshold between the low and medium potentially dangerous glacial lakes should be the mean value between class 1 and 4 (0.325, Table 8). We evaluated the weighting and classification scheme based on visual interpretation of the morphometric variables and the satellite imagery of selected case studies, previous GLOF events and knowledge from field visits from the authors and their colleagues from the Institute of Geography, Almaty and the State Agency for Mudflow Protection of the Ministry of Emergency Situations of the Republic of Kazakhstan (Kazselezashchita). We focused on the identified lakes with a high danger and its surrounding lakes.

4 Results

4.1 Glacial lakes and its changes

Overall, 66 lakes were identified in the imagery of the 1970s, while this number had increased to 132 in 2007 (Table 7). The number of the lakes almost doubled between 1972 and 2000 while it remained nearly constant between 2000 and 2007. Twelve of the lakes showed no significant changes over the investigated period. The two largest lakes are Bolshoje Almatinskoje lake and lake Dzhazil–Köl. The former, which is close to Almaty, developed after a rock avalanche and is now dammed by an artificial dam. The latter, situated at the end of Chon–Kemin valley, is dammed by two joining rock glaciers. About 60% of the identified lakes are in direct contact with the glacier ice. The overall area of the lakes increased from about 2.56 km^2 to about 3.44 km^2 and the estimated volume from $\sim 42.4 \times 10^6$ m^3 to $\sim 50.1 \times 10^6$ m^3 (1972–2007). Both the absolute lake area and the change rate increased from the periods 1972–2000 to 2000–2007. However, during this time it is observed that several lakes also lost surface area or disappeared completely. This is likely to be caused by lake drainages some of which may have occurred rapidly causing a GLOF, as e.g. in Kishi Almaty (Malaya Almatinka) valley in 1973 (Popov 1988).

4.2 Potentially dangerous glacial lakes (PDGL)

The results of the hazard assessment showed that the majority of the lakes are classified as 'low danger' (Table 8; Fig. 6). These lakes are usually small and did not change significantly over the time. Overall, 47 out of 132 lakes are mapped in 2007 and are falling within the high and medium danger category. There is a medium to high possibility of an outburst of these lakes that can affect infrastructures or human beings. Therefore, these lakes should be studied and monitored more in detail. In the following section, we describe the situation of identified two highly dangerous lakes and some further lakes as case studies.

The lake identified as the highest danger is Lake No. 23 [named Lake No. 6 in the local literature, e.g. Kasatkin and Kapista (2009)] and situated in Kishi Almaty (Malaya

Table 7 Number, area and the estimated volume and its changes of the glacial lakes in the study area for 1972, ~1999 and ~2007

	1972	2000	2007	1972–2000		2000–2007		1972–2007	
				Δ	Δ/a	Δ	Δ/a	Δ	Δ/a
Number	66	127	132	+61	+2.26	+5	+0.5	+65	+1.86
Area (km^2)	2.56 ± 0.14	3.28 ± 0.17	3.44 ± 0.18	+0.72 ± 0.22	+0.027 ± 0.008	+0.12 ± 0.24	+0.015 ± 0.03	+0.88 ± 0.23	+0.025 ± 0.007
Volume[a] ($\times 10^6$ m^3)	42.4 ± 10.6	47.2 ± 11.8	50.1 ± 12.5	+4.8 ± 15.9	+0.17 ± 0.57	+2.9 ± 17.2	+0.41 ± 2.46	+7.7 ± 16.4	+0.22 ± 0.47

[a] We included an additional uncertainty of 20% in the lake volume calculation (see text)

Table 8 Numbers of glacial lakes in each class

Class	Risk index	No. of lakes
I (very low danger)	≤0.1	6
II (low danger)	0.1–0.325	79
III (medium danger)	0.325–0.574	45
IV (high danger)	>0.574	2

Almatinka) valley which is close to the Million City of Almaty and was identified as highly dangerous (Figs. 7e, 8a). It is in close contact to a steep glacier and grew significantly since the 1970s. We modelled a high danger of ice avalanches or rock falls into the lake. Permafrost is likely to be in the dam and, in addition, the outburst modelling shows a high probability of a mudflow. And in fact this lake was also identified by the State Agency for Mudflow Protection of the Ministry of Emergency Situations of the Republic of Kazakhstan (Kazselezashchita) as a highly dangerous lake (Popov 1988; Kasatkin and Kapista 2009; Tokmagambetov 2009). This lake has formed in 1959 and increased concomitantly with the shrinkage of the adjacent Manshuk Mametova Glacier at the altitude of 3,600 m. Its tongue retreated approximately 250 m since 1958. By the end of the 1990s, the lake had a length of 230 m, a width of 150 m, and the area reached 24,000 m^2 with a volume close to 250,000 m^3. It is estimated that an outburst would cause a mudflow with a volume of more than 2 million m^3. Kazselezashchita built a channel in the dam to decrease of the mudflow danger in 1997. Therefore, the lake volume decreased up to 150 thousand m^3. However, by the year 2010 because of melting of ice, the average depth of the lake increased again and reached a maximum depth of 22 m, and the volume again reached 250,000 m^3. Therefore, Kazselezashchita has deepened the channel which has lowered a water level on 6.6 m to a volume slightly higher than 100,000 m^3.

The second highly dangerous lake, Lake No. 122, is situated in a side valley of the Chon–Kemin river (Fig. 7a). The lake is in direct contact to a glacier which has not only retreated but has also a very flat tongue which makes a further growth of the lake very likely. In addition, the lake has adjacent steep slopes and is exposed to both ice and rock avalanches. It is anticipated that no settlements would be affected by an outburst. However, there is a possibility that the gravel road that connects the Issyk–Kul with Almaty and which is frequently used by tourists and trekkers might be destroyed. Similarly, the neighbouring lake has a medium risk. It has similar conditions but is much smaller and the lake growth is slower. An example for a medium dangerous lake is No. 67 situated at south of the Shilek (Chilik) river (7B). The parent glacier shows characteristics for increasing the outburst hazard of the glacial lake, such as strong recession and flat snout. In addition, the lake area has increased by about 40% between 1999 and 2007. However, the affected area of an outburst will be probably small as the overall slope is gentle.

The characteristics of Lake No. 36 which was classified as medium dangerous and situated at the end of Levij Talgar valley are similar to those of Lake No. 67 (Fig. 7c). In addition, it is comparatively large. Permafrost thaw might destabilise the moraine dam. However, the dam is relatively wide. A new lake has developed up-valley which can, in case of an outburst, trigger the overflow of Lake No. 36. Hence, this lake should be continuously monitored also because Levij Talgar valley is frequently visited by tourists and an outburst in this valley can destroy infrastructures at the foothills such as in the case of the 2003 outburst event (Bolch 2008). Another larger lake (No. 22) in this valley is

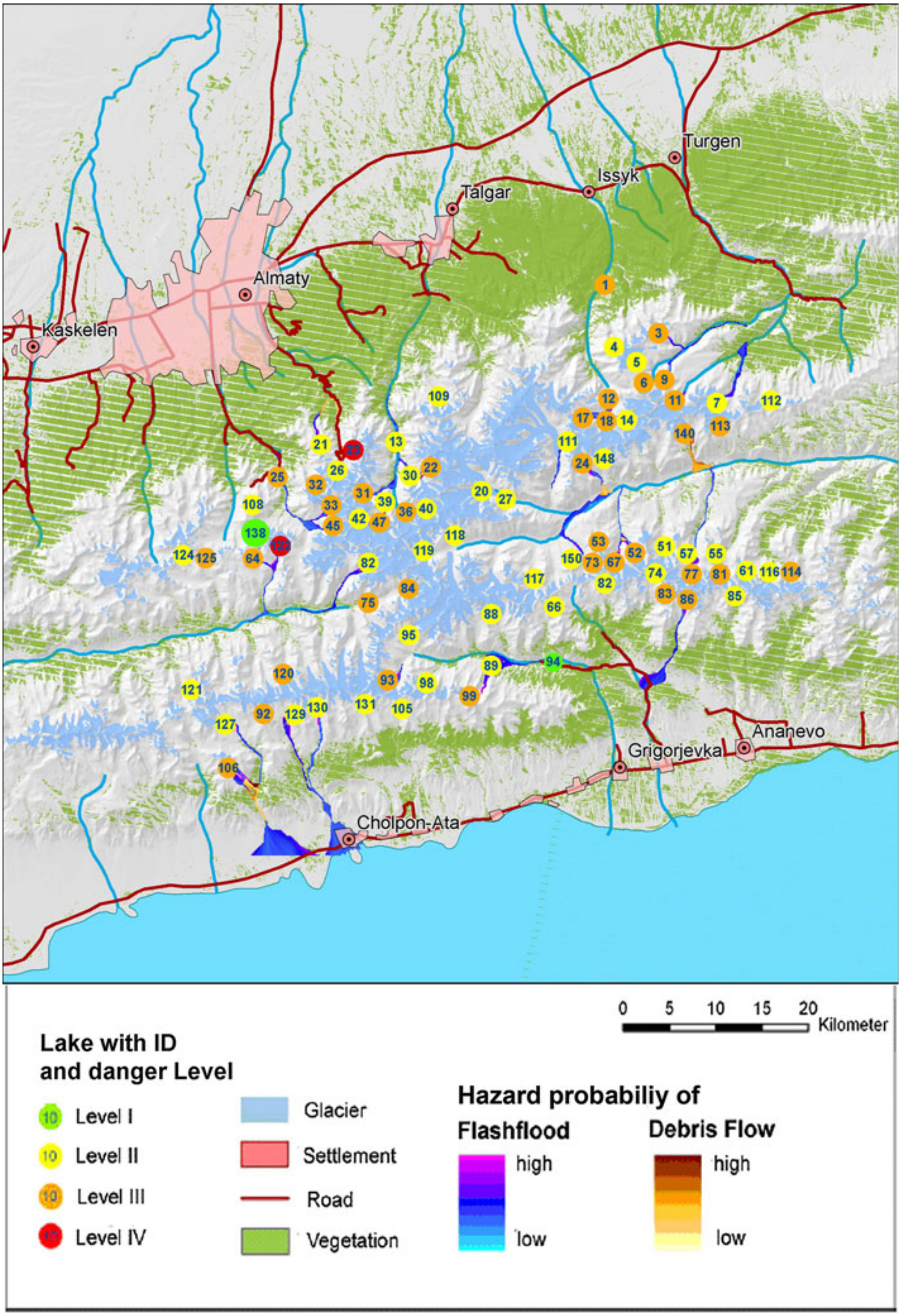

Fig. 6 The location of potentially dangerous glacial lakes in the study area of northern Tien Shan

classified as a medium risk (7D). This seems reasonable as it is not adjacent to a glacier and mass movements will not reach the lake. Another example of medium risk is Lake No. 93 in Chon Aksu valley (Fig. 8b), although the lake did not grow significantly over the

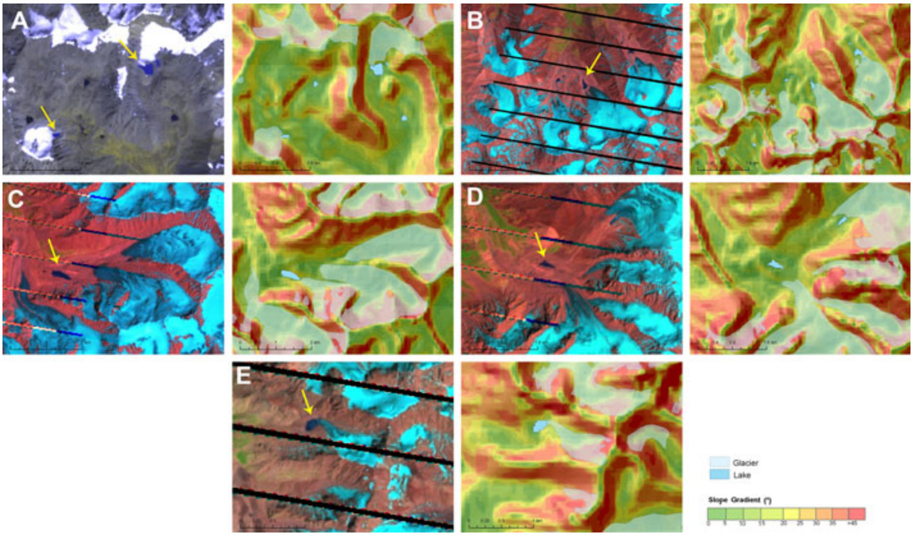

Fig. 7 Visualisation of the situation of selected glacial lakes. For each example, we show a satellite image and the slope of the topography. The *arrow* indicates a lake

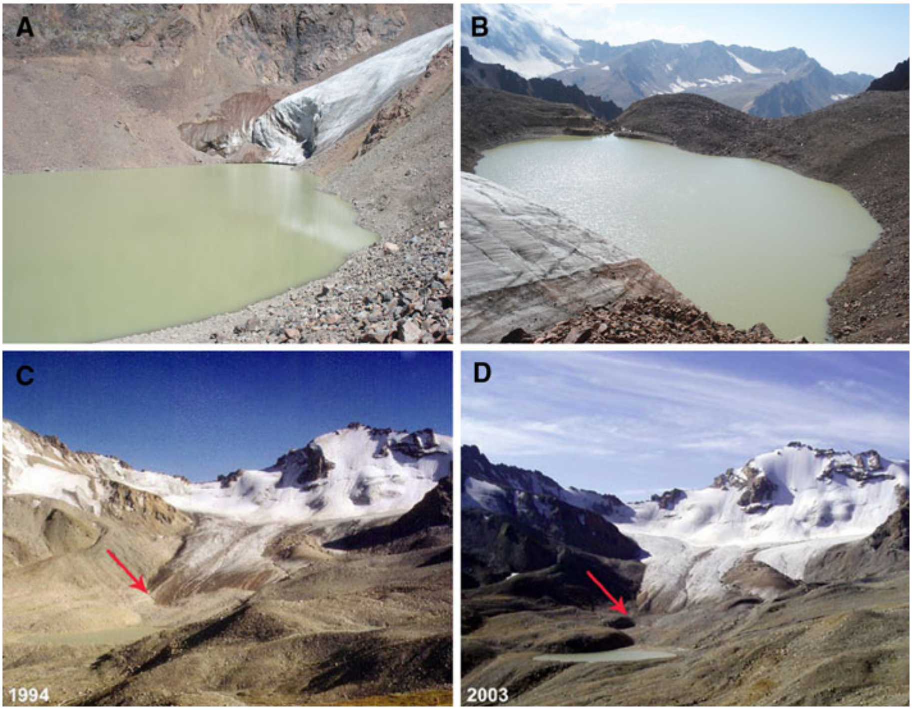

Fig. 8 Two examples of glacial lakes in the Northern Tien Shan. *Top* The highly dangerous lake No. 23 (Nr. 6 of the valley) in Kishi Almaty (Malaya Almatinka) valley after the surface lowering by deepening of the outflow channel in 2010 (**a** view from dam to glacier, **b** view to dam, photos: Blagoveshchenskiy), *bottom* Lake No. 22 in Chon Aksu valley in 1994 (**c** photo: D. Wagner) and 2003 (**d** photo: T. Bolch)

observed period. The dam could be affected by permafrost thaw and an outburst would trigger a flash flood.

5 Discussion

5.1 Glacial lakes in northern Tien Shan

Previous studies have shown that the number and the area of glacial lakes have increased concomitantly in terms of glacier shrinkage in many regions (Bajracharya and Mool 2009; Gardelle et al. 2011). The susceptibility of a lake outburst increases when the thawing of permafrost destabilises the moraine dam or if the glacial lake is growing (Richardson and Reynolds 2000). Temperatures in northern Tien Shan have increased about 0.8 K/100a between the period 1900–2000 and about 2.0 K/100a on average for the second half of the last century (Giese et al. 2007; Bolch 2007). The increase was found to be less pronounced in the mountainous areas, but is still obvious. No significant trend was found with the precipitation (Aizen et al. 1997; Bolch 2007). The glaciers in the study area are shrinking concomitantly with respect to the climate change. The glacier shrinkage at the northern edge of the Tien Shan is more pronounced than the central parts with its continental mountain ranges (Aizen et al. 2006; Bolch 2007; Kutuzov and Shahgedanova 2009; Narama et al. 2010b; Solomina et al. 2004). The lower boundary of permafrost has shifted upwardly about 150–200 m since the beginning of the 20th century while the area of permafrost has decreased by approximately 18% (Marchenko et al. 2007). Hence, it could be expected that the number and area of potentially dangerous lakes increases in the study area, a fact which is confirmed by this study. Other studies on glacial lakes in the same and adjacent mountain ranges of the Tien Shan show similar results (Erohin and Cerny 2009; Janský et al. 2011; Narama et al. 2009, 2010a; Popov 1988). Further glacier shrinkage will probably lead to higher danger of a GLOF. Also in the past, several glacial lake outburst events were caused by rapid glacier shrinkage followed by an overflow of the moraine dam.

The national scientists and the responsible authorities in Kazakhstan and Kyrgyzstan have been well aware of the glacial lake hazards for several decades. Different hazard mitigation activities such as the activities for the lowering of the lake levels (e.g. Kasatkin and Kapista 2009; Popov 1988), mudflow protection walls and dams (such as in Kishi and Ulken Almatinka valleys, Yegorov 2007) reduced the risk significantly. However, GLOFs and mudflows still occur and can endanger infrastructures. This is especially true for areas above the protection walls and dams.

5.2 Methodology

The case studies show that our suggested approach which is based on remote sensing analysis and modelling can be successfully applied to identify potentially dangerous glacial lakes. It is hence, suitable for a first comprehensive assessment of PDGLs for a larger area and addresses the levels 1 and 2 of the suggested approach by Huggel et al. (2002). We combined the manifold conditioning parameters which had not been addressed previously in this comprehensive way. The approach is easily reproducible as it is based on well-developed methods such as the detection of water bodies using multispectral imagery (Huggel et al. (2002), automated detection of glaciers (Bolch and Kamp 2006; Paul et al. 2002), and their velocities (Bolch et al. 2008; Kääb 2005) and simple but robust models such as the modelling of an outburst path or rock/ice avalanches (Huggel et al. 2003), or a permafrost model (Keller 1992). Older panchromatic imagery such as Corona proved to be suitable to extend the analysis back in time which was already shown for glaciers (Narama et al. 2010b; Bolch et al. 2010). It could also be demonstrated that it is possible to detect PDGLs for a larger area such as mountain ranges covering a whole Landsat scene ($\sim$185 by 185 km) within a short period of time. However, the results need to be carefully evaluated and the weighting scheme possibly adjusted for the special situation in the respective study region. Data from former outburst events are valuable sources for calibration. In case of the current study area, they confirmed the importance of lake growth and the possibility of existing ice in the moraine dam.

The three main limitations of the geomatics-based approach are that (1) the dam characteristics and the probability of a dam failure can only be addressed marginally, (2) lakes in shaded areas and turbid lakes are difficult to identify automatically, (3) the modelling was based on the SRTM3 DEM with a spatial resolution of $3'$. The result of the modelling of the outburst path is based on the SRTM DEM which highlights the most endangered areas. Comparisons with historical outbursts show that the path length and, hence, the affected areas are underestimated. For instance, a flash flood caused by a lake outburst which happened in 2003 in Leviy Talgar valley after heavy rainfalls destroyed a bridge at the foothills but the modelled flow path stopped shortly before this point. Similar uncertainty exists in the modelling of the mass movements based on the SRTM. Hence, the SRTM3 DEM proved to be suitable for a first assessment but has inaccuracies which were also concluded by Frey et al. (2010b). A more accurate DEM should be used if available.

The major limitation of a remote sensed based study is that the characteristics and stability of the moraine/lake dam cannot or only roughly taken into account. The used permafrost model is coarse and does not consider the material composition which can strongly alter the thermal conditions within the materials and also retard the thawing of the ice. However, this model can be easily applied to other mountainous regions in order to provide a first hint about the existence of permafrost. In addition, this model can be applied for estimation of the future permafrost extent and to address the danger of increased mass movements due to permafrost thaw. Other critical measures of the stability of the dam are the types of drainage. While the drainage over the dam could be detected at least with using high resolution imagery outflows under or through the dam or piping cannot be addressed. A further limitation is that the water volume of the lakes can only be roughly calculated based on the area. Field investigations would be necessary to measure the lake depth and to address the grain size distribution of the moraine.

The applied methodology for the categorisation of the glacial lakes produced reasonable results. The utilised weighting according to the importance of the variables, however, should be carefully chosen by an expert and adjusted to the study region.

6 Conclusion

The presented geomatics-based approach successfully detects potentially dangerous glacial lakes across a larger area and presents decision criteria where time- and cost-intensive field studies should be performed. The availability of data from previous outburst events helps to adjust the weighting scheme for the respective study region. The main drawback is that the stability of the moraine can currently only roughly be addressed by remote sensing and modelling. The nearly globally available SRTM DEM is a good choice for the first assessment but a more accurate DEM of higher resolution should be utilised for the analysis if available.

We detected two highly dangerous lakes which should be continuously monitored. For these lakes and lakes of medium danger which could affect infrastructures and endanger human lives (e.g. at the northern slope of Ile Alatau and the southern slope of Kungey Alatau and in the mountains along trekking routes) visual checking and manual interpretation are needed. Continuous climate warming and the resultant permafrost thaw and glacier recession will increase the potential danger of lake outbursts.

Acknowledgments The authors would like to thank D. Quincey and C. Huggel for their thorough comments which significantly improved the quality of the manuscript. The logistic support by I. Severskiy, I. Shesterova and A. Kokarev (Institut for Geography, Almaty) is appreciated.

References

Aizen VB, Aizen EM, Melack JM, Dozier J (1997) Climate and hydrologic changes in the Tien Shan, central Asia. J Clim 10:1393–1404

Aizen VB, Kuzmichenok VA, Surazakov AB, Aizen EM (2006) Glacier changes in the central and northern Tien Shan during the last 140 years based on surface and remote-sensing data. Ann Glaciol 43:202–213

Alean J (1985) Ice avalanches: some empirical information about their formation and reach. J Glaciol 31:324–333

Allen SK, Schneider D, Owens IF (2009) First approaches towards modelling glacial hazards in the Mount Cook region of New Zealand's Southern Alps. Nat Hazard Earth Syst Sci 9(2):481–499

Baimoldayev T, Vinohodov V (2007) Kazselezashchita–operativnye mery do I posle stihii–Izd. Bastau, Almaty, p 284

Bajracharya SR, Mool PK (2009) Glaciers, glacial lakes and glacial lake outburst floods in the Mount Everest region, Nepal. Ann Glaciol 50(53):81–86

Berry PA, Garlick JD, Smith RG (2007) Near-global validation of the SRTM DEM using satellite radar altimetry. Remote Sens Environ 106(1):17–27

Berthier E, Vadon H, Baratoux D, Arnaud Y, Vincent C, Feigl KL, Rémy F, Legrésy B (2005) Surface motion of mountain glaciers derived from satellite optical imagery. Remote Sens Environ 95(1):14–28

Blagoveshchenskiy VP, Yegorov AB (2009) The Ile Alatau range natural hazards. In: Materials of the International Conference "Mitigation of natural hazards in mountain areas", 15.–18.9.2009, Bishkek, pp 153–157

Böhner J (1996) Säkulare Klimaschwankungen und rezente Klimatrends Zentral- und Hochasiens. Göttinger Geographische Abhandlungen 101, pp 166

Bolch T (2007) Climate change and glacier retreat in northern Tien Shan (Kazakhstan/Kyrgyzstan) using remote sensing data. Glob Planet Change 56:1–12

Bolch T (2008) Klima- und Gletscheränderungen im nördlichen Tien Shan (Kasachstan/Kyrgyzstan) mit einem Vergleich zur Bernina-Gruppe/Alpen (in German with English and Russian abstract and captions). VDM Verlag Dr. Müller, p 264, ISBN: 3-639-03742-1. (=Bolch, T. (2006): Dissertation, Universität Erlangen-Nürnberg, p 210. http://www.opus.ub.uni-erlangen.de/opus/volltexte/2006/447/)

Bolch T, Kamp U (2006) Glacier mapping in high mountains using DEMs, landsat and ASTER data, Grazer Schriften der Geographie und Raumforschung. In: Proceedings 8th Int. Symp. on high mountain remote sensing cartography, vol 41, 20–27 March 2005, La Paz, Bolivia, pp 13–24

Bolch T, Kamp U, Olsenholler J (2005) Using ASTER and SRTM DEMs for studying geomorphology and glaciation in high mountain areas. In: Oluic M (ed) New strategies for European remote sensing. Millpress, Rotterdam, pp 119–127

Bolch T, Buchroithner MF, Kunert A, Kamp U (2007) Automated delineation of debris-covered glaciers based on ASTER data. In: Gomarasca MA (ed) GeoInformation in Europe (=Proc. 27th EARSeL-Symposium, 4.-7.6.07, Bozen, Italy). Millpress, Netherlands, pp 403–410

Bolch T, Buchroithner MF, Bajracharya SR, Peters J, Baessler M (2008) Identification of glacier motion and potentially dangerous glacier lakes at Mt. Everest area/Nepal using spaceborne imagery. Nat Hazard Earth Syst Sci 8(6):1329–1340

Bolch T, Yao T, Kang S, Buchroithner MF, Scherer D, Maussion F, Huintjes E, Schneider C (2010) A glacier inventory for the western Nyainqentanglha range and Nam Co Basin, Tibet, and glacier changes 1976–2009. Cryosphere 4:419–433

Bolch T, Pieczonka T, Benn DI (2011) Multi-decadal mass loss of glaciers in the Everest area (Nepal, Himalaya) derived from stereo imagery. Cryosphere 5:349–358

Buchroithner M (1996) Jökulhlaup mapping in the Himalaya by means of remote sensing. Kartographische Bausteine 12:75–86

Buchroithner M, Jentsch G, Wanivenhaus B (1982) Monitoring of recent geological events in the Khumbu area (Himalaya, Nepal) by digital processing of Landsat MSS data. Rock Mech 15:181–197

Chedija OK (1986) Morfostruktury i novejzhij Tektogenez Tjan-Shanja, Ilm, Frunse

Clague JJ, Evans SG (2000) A review of catastrophic drainage of moraine-dammed lakes in British Columbia. Quat Sci Rev 19:1763–1783

Dashora A, Lohani B, Malik JN (2007) A repository of earth resource information—CORONA satellite programme. Curr Sci 92(7):926–932

Delevaux D, Abdrakhmatov KE, Lemzin IN, Strom L (2001) Opolszni i Razpyvy Keminskogo Zemletrjacenija 1911 g. s Ms 8, 2 v Kirgizii. Geologija i Geofisika 42(10):1667–1677

Erohin S, Cerny M (2009) Monitoring of out bursting lakes of Kyrgyzstan. In: Material of the international conference “Mitigation of natural hazards in mountain areas”, 15.–18.9.2009, Bishkek, pp 30–34

Falorni G, Teles V, Vivoni ER, Bras RL, Amartunga KS (2005) Analysis and characterization of the vertical accuracy of digital elevation models from the shuttle radar topography mission. In J Geophys Res 110 (F02005). doi:10.1029/2003JF000113

Frey H, Huggel C, Paul F, Haeberli W (2010a) Automated detection of glacier lakes based on remote sensing in view of assessing associated hazard potentials. In: Kaufmann V, Sulzer W (eds) Proc. 10th international symposium on high mountain remote sensing cartography. Grazer Schriften der Geographie und Raumforschung, vol 45, pp 261–272

Frey H, Haeberli W, Linsbauer A, Huggel C, Paul F (2010b) A multi-level strategy for anticipating future glacier lake formation and associated hazard potentials. Nat Hazard Earth Syst Sci 10(2):339–352

Fujita K, Suzuki R, Nuimura T, Sakai A (2008) Performance of ASTER and SRTM DEMs, and their potential for assessing glacial lakes in the Lunana region, Bhutan Himalaya. J Glaciol 54(185):220–228

Gardelle J, Arnaud Y, Berthier E (2011) Contrasted evolution of glacial lakes along the Hindu Kush Himalaya mountain range between 1990 and 2009. Glob Planet Chang 75:47–55

Giese E, Moßig I, Rybski D, Bunde A (2007) Long-term analysis of air temperature trends in Central Asia. Erdkunde 61(2):186–202

Gorbunov AP, Severskiy EV (2001). Seli okrestnostej Almaty. Almaty

Gorbunov AP, Severskiy EV, Titkov SN (1996) Geokriologichesije Uslovija Tjan-Shanja i Pamira, Institut Merzlotovedenija, Rassiyskaja Akademija Nauk, Irkutsk

Gorbunov AP, Marchenko SS, Severskiy EV (2004) The thermal environment of blocky materials in the mountains of Central Asia. Permafr Periglac Process 15(1):95–98

Granshaw FD, Fountain AD (2006) Glacier change (1958–1998) in the North Cascades National Park Complex, Washington, USA. J Glaciol 52(177):251–256

Haeberli W (1983) Frequency and characteristics of glacier floods in the Swiss Alps. Ann Glaciol 4:85–90

Havenith HB, Strom A, Jongmans D, Abdrakhmatov A, Delvaux D, Tréfois P (2003) Seismic triggering of landslides, part A: field evidence from the Northern Tien Shan. Nat Hazard Earth Syst Sci 3(1/2):135

Hsü KJ (1975) Catastrophic debris streams (Sulzstroms) generated by rockfalls. Geol Soc Am Bull 86:129–140

Huggel C, Kääb A, Haeberli W, Teysseire P, Paul F (2002) Remote sensing based assessment of hazards from glacier lake outbursts: a case study in the Swiss Alps. Can Geotech J 39:316–330

Huggel C, Kääb A, Haeberli W, Krummenacher B (2003) Regional-scale GIS-models for assessment of hazards from glacier lake outbursts: evaluation and application in the Swiss Alps. Nat Hazard Earth Syst Sci 3:647–662

Huggel C, Zgraggen-Oswald S, Haeberli W, Kääb A, Polkvoj A, Galushkin I, Evans SG (2005) The 2002 rock/ice avalanche at Kolka/Karmadon, Russian Caucasus: assessment of extraordinary avalanche formation and mobility, and application of QuickBird satellite imagery. Nat Hazard Earth Syst Sci 5:173–187

Ives J (1986) Glacial lake outburst floods and risk engineering in the Himalaya. ICIMOD, Kathmandu

Iwata S, Ageta Y, Naito N, Sakai A, Narama C, Karma (2002) Glacial lakes and their outburst flood assessment in the Bhutan Himalaya. Glob Environ Res 6(1):3–17

Janský B, Sobr M, Engel Z (2011) Outburst flood hazard: case studies from the Tien-Shan Mountains, Kyrgyzstan. Limnologica—Ecology and Management of Inland Waters. doi:10.1016/j.limno.2009.11.013

Kääb A (2005) Combination of SRTM3 and repeat ASTER data for deriving alpine glacier flow velocities in the Bhutan Himalaya. Remote Sens Environ 94:463–474

Kääb A, Huggel C, Fischer L, Guex S, Paul F, Roer I, Salzmann N, Schlaefli S, Schmutz K, Schneider D, Strozzi T, Weidmann Y (2005) Remote sensing of glacier- and permafrost-related hazards in high mountains: an overview. Nat Hazard Earth Syst Sci 5:527–554

Kahle E (1998) Betriebswirtschalftliche Entscheidungen: Lehrbuch zur Einführung betreibswirtschaftlicher Entscheidungstheorie. München

Kaibori M, Sassa K, Tochiki S (1988) Betrachtung über die Bewegung von Absturzmaterialien. International Symposium of INTERPRAEVENT 1988/07, vol 2, pp 227–242

Kamp U, Bolch T, Olsenholler J (2005) Geomorphometry of Cerro Sillajhuay, Chile/Bolivia: comparison of DEMs derived from ASTER remote sensing data and contour maps. Geocarto Int 20(1):23–34

Kasatkin NE, Kapista VP (2009) The morainic lakes dynamics in the Ile Alatau. In: Materials of the Internat. Conf. "Mitigation of natural hazards in mountain areas", 15.–18.9.2009, Bishkek, pp 55–58

Keller F (1992) Automated mapping of mountain permafrost using the program PERMAKART within the geographical information system ARC/INFO. Permafr Periglac Process 3(2):133–138

Kocak G, Büyüksalih G, Jacobsen K (2004) Analysis of digital elevation models determined by high resolution space images. In Int Arch Photogramm Remote 35(B4):636–641

Korjenkov AM, Kovalenko VA, Usmanov SF (2004) Long-term preservation of Paleoseismic deformation as a tool for revealing traces of ancient seismic catastrophes (example of the Chon-Kemin Valley, Kyrgyzstan). Kartographische Bausteine 28:137–154

Kutuzov S, Shahgedanova M (2009) Glacier retreat and climatic variability in the eastern Terskey-Alatoo, inner Tien Shan between the middle of the 19th century and beginning of the 21st century. Glob Planet Change 69(1–2):59–70

Leprince S, Barbot S, Ayoub F (2007) Automatic and Precise Orthorectification, Coregistration, and Subpixel correlation of satellite images, application to ground deformation measurements. IEEE Trans Geosci Remote Sens 45(6):1529–1558

Luckman A, Quincey D, Bevan S (2007) The potential of satellite radar interferometry and feature tracking for monitoring flow rates of Himalayan glaciers. Remote Sens Environ 111:172–181

Lukk AA, Yunga S, Shevchenko VI, Hamburger MW (1995) Earthquake focal mechanisms, deformation state and Seismotektoniks of the Pamir-Tien Shan region, Central Asia. J Geophys Res 100(B100):20321–20343

Ma D, Tu J, Cui P, Lu R (2004) Approach to mountain hazards in Tibet, China. J Mt Sci 1(2):143–154

Marchenko SS (1999) Sovremennoje i ozhidaemje v 21. V. izmenenije merzlotno-klimaticheskikh uslovnij b severnom Tjan-Shanje. Criosfera Semli 3(2):13–21

Marchenko SS (2001) A model of permafrost formation and occurrences in the intracontinental mountains. Norsk Geograf Tidsskrift 55(4):230–234

Marchenko SS, Gorbunov AP, Romanovsky VE (2007) Permafrost warming in the Tien Shan Mountains, Central Asia. Glob Planet Change 56(3–4):311–327

Medeuov AR, Nurlanov MT (1996) Selevye Javlenija seismoaktivnykh Territorij Kazakhstana. Akademiya Nauk, Almaty

Medeuov A, Kolotilin NF, Keremkulov VA (1993) Seli Kazakhstana. Gylym, Almaty, p 160

Mergili M, Schneider D, Worni R, Schneider J (2011) Glacial lake outburst floods in the Pamir of Tajikistan: challenges in prediction and modelling. In 5th International Conference on Debris-Flow Hazards Mitigation: Mechanics, Prediction and Assessment, University of Padova, Italy, 14-17.06.11, accepted

Narama C, Severskiy I, Yegorov A (2009) Current state of glacier changes, glacial lakes, and outburst floods in the Ile Ala-Tau and Kungoy Ala-Too ranges, northern Tien Shan Mountains. Ann Hokkaido Geogr 84:22–32

Narama C, Duishonakunov M, Kääb A, Daiyrov M, Abdrakhmatov K (2010a) The 24 July 2008 outburst flood at the western Zyndan glacier lake and recent regional changes in glacier lakes of the Teskey Ala-Too range, Tien Shan, Kyrgyzstan. Nat Hazard Earth Syst Sci 10:647–659

Narama C, Kääb A, Duishonakunov M, Abdrakhmatov K (2010b) Spatial variability of recent glacier area changes in the Tien Shan Mountains, Central Asia, using Corona (1970), Landsat (2000), and ALOS (2007) satellite data. Glob Planet Change 71(1–2):42–54

Passmore DG, Harrison S, Winchester V, Rae A, Severskiy IV, Pimankina NV (2008) Late Holocene debris flows and valley floor development in the Northern Zailiiskiy Alatau, Tien Shan Mountains, Kazakhstan. Arctic. Antarct Alp Res 40(3):548–560

Paul F, Kääb A, Maisch M, Kellenberger T, Haeberli W (2002) The new remote sensing derived swiss glacier inventory: I. Methods. Ann Glaciol 34:355–361

Plehanov PA, Sudakov PA, Tokmagambetov GA (1975) Prichiny obrazovaniya I processy formirovaniya selevogo potoka na reke Malaya Almatinka 15 iyulya 1973 g. Vestnik AN KazSSR 4:24–25

Popov NV (1984a) O seleopasnyh ozerah glacialnoi zony Zailiyskogo Alatau. Problemy protivoselevyh meropriy. Alma-Ata:96–105

Popov NV (1984b) O glyacialnom selevom potoke 23 Iyulya, 1980 goda v basseine reki Kaskelen Zailiyskogo Alatau. Problemy protivoselevyh meropriyatiy. Alma-Ata:222–230

Popov NV (1988) Die Kontrolle gefährlicher Gletscherseen im nördlichen Tienschan. In: Proceedings of the International Symposium Interpraevent, vol 4, pp 29–41

Quincey DJ, Lucas RM, Richardson SD, Glasser NF, Hambrey MJ, Reynolds JM (2005) Optical remote sensing techniques in high-mountain environments: application to glacial hazards. Prog Phys Geogr 29(4):475–505

Quincey DJ, Richardson SD, Luckman A, Lucas RM, Reynolds JM, Hambrey MJ, Glasser NF (2007) Early recognition of glacial lake hazards in the Himalaya using remote sensing datasets. Glob Planet Change 56(1–2):137–152

Reynolds JM (2000) On the formation of supraglacial lakes on debris-covered glaciers. IAHS Publication, vol 264 (= Debris-covered Glaciers), pp 153–161

Richardson SD, Reynolds JM (2000) An overview of glacial hazards in the Himalayas. Quat Int 65/66(1):31–47

Salzmann N, Kääb A, Huggel C, Allgöwer B, Haeberli W (2004) Assessment of the hazard potential of ice avalanches using remote sensing and GIS-modelling. Norsk Geograf Tidsskrift 58:74–84

Scherler D, Leprince S, Strecker MR (2008) Glacier-surface velocities in alpine terrain from optical satellite imagery—accuracy improvement and quality assessment. Remote Sens Environ 112(10):3806–3819

Schneider JF (2004) Risk assessment of remote geohazards in western Pamir, GBAO, Tajikistan. In: Proceedings of the international conference on high mountain hazard prevention, Vladikavkaz Moscow, 23–26.06. 2004, pp 252–255

Severskiy IV, Zichu X (eds) (2000) Snow cover and avalanches in the Tien Shan Mountains. Almaty, VAC Publishing House, Almaty

Shusharin VI, Popov NV (1981) Razvitie selevogo potoka v basseine reki Sredniy Talgar.—problemy protivoselevyh meropriyatiy. Alma-Ata:153–157

Solomina ON, Barry R, Bodnya M (2004) The retreat of Tien Shan glaciers (Kygryzstan) since the Little Ice age estimated from aerial photographs, lichenometric and historical data. Geograf Ann Ser A 86(2):205–216

Storm AL, Korup O (2006) Extremly large rockslides and rock avalaches in the Tien Shan Mountains, Kyrgyzstan. Landslides 3:125–136

Tokmagambetov TG (2009) The moraine-dammed glacial lakes current state in the Iliy Alatau. In: Materials of the International conference on "Mitigation of natural hazards in mountain areas", 15–18.9.2009, Bishkek, pp 82–83

Utirov CU (1978) Seismic deformations. Geological principles of the seismic zoning of the Issuk-Kul depression. Ilm, Frunze, pp 91–111

Vuichard D, Zimmermann M (1987) The 1985 catastrophic drainage of a moraine-dammed lake, Khumbu Himal, Nepal: cause and consequences. Mt Res Dev 7:91–110

Wessels R, Kargel J, Kieffer H (2002) ASTER measurement of supraglacial lakes in the Mount Everest region of the Himalaya. Ann Glaciol 34:399–408

Woerd J, van der Owen LA, Tapponnier P, Xu X, Kervyn F, Finkel RC, Barnard PL (2004) Giant, _M8 earthquaketriggered ice avalanches in the eastern Kunlun Shan, northern Tibet: characteristics, nature and dynamics. Geol Soc Am Bull 116(3):394–406

Yadav RR, Kulieshhius P (1992) Dating of Earthquakes: tree ring responses to the catastrophic Earth Quake of 1887 in Alma Ata, Kasakhstan. Geograph J 158:295–299

Yegorov A (2007) Analyse und Bewertung von Naturgefahren als Grundlage für ein nachhaltiges Naturgefahrenmanagment in Gebirgssystemen SO-Kasachstans am Beispiel des Ile-Alatau. Dissertation, LMU München